JAERI-M
9945

THERMAL AND STRUCTURAL DESIGN STUDY OF DIVERTOR COLLECTOR PLATES

January 1982

Kazunori KITAMURA*, Hiromasa IIDA and Kiyoshi SAKO

日本原子力研究所
Japan Atomic Energy Research Institute

JAERI-Mレポートは，日本原子力研究所が不定期に公刊している研究報告書です。
入手の問合わせは，日本原子力研究所技術情報部情報資料課（〒319-11茨城県那珂郡東海村）あて，お申しこしください。なお，このほかに財団法人原子力弘済会資料センター（〒319-11 茨城県那珂郡東海村日本原子力研究所内）で複写による実費頒布をおこなっております。

JAERI-M reports are issued irregularly.
Inquiries about availability of the reports should be addressed to Information Section, Division of Technical Information, Japan Atomic Energy Research Institute, Tokai-mura, Naka-gun, Ibaraki-ken 319-11, Japan.

編集兼発行　日本原子力研究所
印　　刷　㈱高野高速印刷

JAERI-M 9945

Thermal and Structural Design Study of Divertor Collector Plates

Kazunori KITAMURA*, Hiromasa IIDA
and Kiyoshi SAKO

Division of Thermonuclear Fusion Research,
Tokai Research Establishment, JAERI

(Received January 18, 1982)

Thermal and structural design study of divertor collector plates for a Swimming Pool Type Tokamak Reactor (SPTR) is carried out. Co-axial tube type divertor plate is employed for the reduction of electromagnetic force caused by plasma disruption. Maximum heat flux on cooling surface is sufficiently below burn-out heat flux. High thermal stress appers at the brazing region between copper cooling tube and tungsten armor. Some measures are required to decrease the thermal stress for extending the life time of the plate. These will be decreasing the heat flux on the plate by the reduction of beam angle to the plate or promoting the boiling in the tube by the reduction of coolant pressure.

The life time of the plate by erosion due to ion sputtering is estimated to be about 4 years.

Keywords : Swimming Pool Type Tokamak Reactor, Divertor Collector Plates, Co-axial Tube Assembly, Tungsten Armor, Copper Tube, Forced-convection Surface Boiling, Burn-out Heat Flux, Erosion, Ion Sputtering

---

* On leave from Toshiba Corporation, Yokohama, Japan

JAERI−M 9945

ダイバータ板の熱・構造設計

日本原子力研究所東海研究所核融合研究部

喜多村 和 憲*・飯 田 浩 正・迫　　淳

（１９８２年１月１８日受理）

国内次期装置の一候補であるスイミングプール型トカマク炉のダイバータ板について熱・構造設計を行なった。ダイバータ板はプラズマディスラプション時の電磁力を低減するため二重管構造を採用した。

冷却表面の最大熱流束はバーンアウト熱流束を十分下回り，熱的には問題なかった。機械的強度面では，冷却管（銅）のアーマー材（タングステン）接続部に過大な熱応力が発生する。熱応力による冷却管寿命を妥当なものに延ばすため，冷却水圧力を下げ，管内沸とうを促進して熱応力を軽減する方法や，ビームとダイバータ板の角度を変え，入射熱流束を低減するような対策が必要である。イオン・スパッタリングによるダイバータ板の寿命は約４年になった。

＊　外来研究員（東 芝）

CONTENTS

目　　次

1. Introduction

A poloidal divertor is said to be a promising method for impurity control and ash-exhaust in a Tokamak fusion reactor.[1] However, there are some severe problems in engineering design of divertor collector plates. Requirements for the thermal and structural design of the divertor plates, are as follows;

① Heat flux from plasma and nuclear heat deposition due to neutron and gamma-ray should be removed sufficiently.

② Heat flux on the cooling surface must be below the burn-out heat flux, though partial boiling can be allowed.

③ The temperature of the cooling tube material (copper) must be below 250°C from the stand point of mechanical strength.

④ Divertor plates should have enough stiffness to endure inner pressure, thermal stress due to the non-uniform temperature difference and electromagnetic force on the plates caused by plasma disruption.

⑤ Divertor plates need to be installed in a reactor with a high accuracy not to produce unnecessary peaking of heat flux.

⑥ Divertor plates will be eroded by ion sputtering but should have a sufficiently long life time.

In this report, we propose the divertor collector plates composed of co-axial tubes assembly and conduct their engineering design study for a Japanese next Tokamak reactor. Figure 1 shows a vertical cross sectional view of the reactor module.[2] The reactor studied here is a Swimming Pool Type Tokamak Reactor (SPTR) which is one of the candidates of the Japanese next Tokamak reactor in JAERI.[3]

2. Configuration of divertor plates

The overall configuration of the divertor collector plates is illustrated in Fig.2.[2] The divertor plate is composed of an assembly of co-axial tubes in order to minimize the area made by electrical loops on the plates. Since magnetic flux on each area encircled by the electrical loop is small, the eddy current induced in the loop in the case of plasma disruption, hence the electromagnetic force, also becomes small.

As shown in Fig.2, the divertor plates are supported by their feeder tubes of coolant and cooling headers which are fixed on the base

1. Introduction

A poloidal divertor is said to be a promising method for impurity control and ash-exhaust in a Tokamak fusion reactor.[1] However, there are some severe problems in engineering design of divertor collector plates. Requirements for the thermal and structural design of the divertor plates, are as follows;

① Heat flux from plasma and nuclear heat deposition due to neutron and gamma-ray should be removed sufficiently.

② Heat flux on the cooling surface must be below the burn-out heat flux, though partial boiling can be allowed.

③ The temperature of the cooling tube material (copper) must be below 250°C from the stand point of mechanical strength.

④ Divertor plates should have enough stiffness to endure inner pressure, thermal stress due to the non-uniform temperature difference and electromagnetic force on the plates caused by plasma disruption.

⑤ Divertor plates need to be installed in a reactor with a high accuracy not to produce unnecessary peaking of heat flux.

⑥ Divertor plates will be eroded by ion sputtering but should have a sufficiently long life time.

In this report, we propose the divertor collector plates composed of co-axial tubes assembly and conduct their engineering design study for a Japanese next Tokamak reactor. Figure 1 shows a vertical cross sectional view of the reactor module.[2] The reactor studied here is a Swimming Pool Type Tokamak Reactor (SPTR) which is one of the candidates of the Japanese next Tokamak reactor in JAERI.[3]

2. Configuration of divertor plates

The overall configuration of the divertor collector plates is illustrated in Fig.2.[2] The divertor plate is composed of an assembly of co-axial tubes in order to minimize the area made by electrical loops on the plates. Since magnetic flux on each area encircled by the electrical loop is small, the eddy current induced in the loop in the case of plasma disruption, hence the electromagnetic force, also becomes small.

As shown in Fig.2, the divertor plates are supported by their feeder tubes of coolant and cooling headers which are fixed on the base

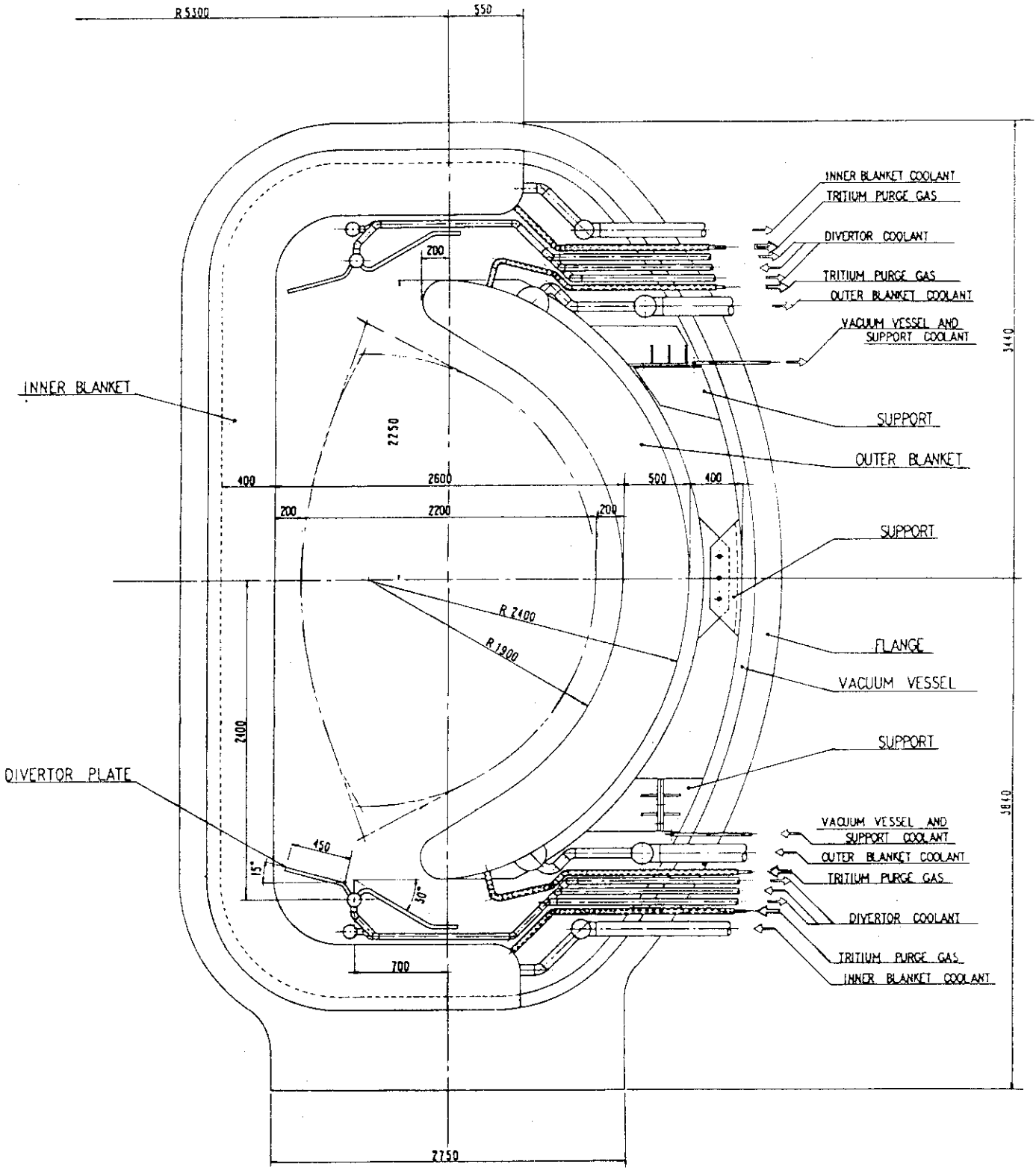

Fig. 1 Vertical cross section view of the reactor module

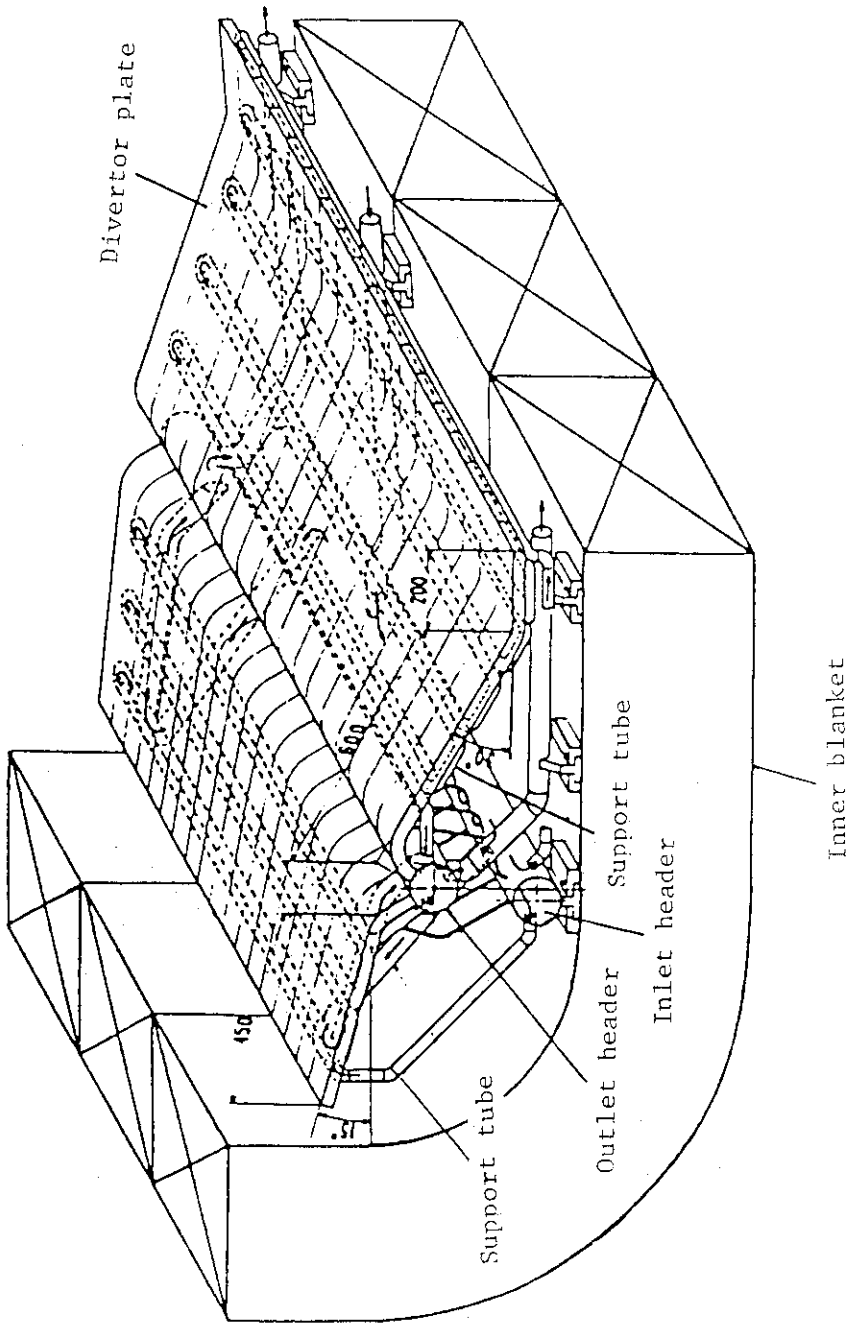

Fig.2 Bird's eye view of divertor collector plate

structures welded on the plasma-side surface of the inner blanket. Void gaps between each pair of adjacent tubes break the electrical circuit. Detailed configuration of the divertor plate is shown in Fig.3.[4] Pressurized water is chosen for the coolant to remove high heat flux on the plate and copper for the tube material to avoid occurrance of large thermal stress. Armor plates made of tungsten with a thickness of 5 mm are attached to the plasma-side surface of the copper tubes to protect the copper tubes from erosion due to ion sputtering. Dimensions of the cooling tubes are determined to be 18 mm inner diameter for the outer tube and 10 mm inner diameter and 12 mm outer diameter for the inner tube, taking into account the pressure drop of the coolant and the realistic fabrication of the tubes. Coolant flows in the inner tube to the end of co-axial tube and returns in the outer tube. The fins between the inner and outer tubes are installed to make the temperature distribution in both the cooling tube and the coolant as uniform as possible. This temperature distribution is caused since heat flux comes from one side.

Stainless steel tubes are placed on the rear side of the tubes in order to prevent protrusion of the tubes from the plate surface and to support the electromagnetic force. These tubes are insulated from the copper tubes electrically.

Armor is brazed to the copper tube in order to efficiently conduct the heat load to the cooling tube. Armor is divided in a longitudinal direction into several sections by grooves for the reduction of thermal stress.

Both the inner and outer divertor plates are inclined to the magnetic line with an angle of 40° for the reduction of maximum heat flux on the plates.

The spatial distributions of the heat flux and particle flux density on the plate normal to the magnetic line at R = 5.3 m is assumed to be Gaussian as follows;

$$q(x) = q_{max} \cdot e^{-\left(\frac{x}{\Delta}\right)^2} \quad . \tag{1}$$

$$\varphi(x) = \varphi_{max} \cdot e^{-\left(\frac{x}{\Delta}\right)^2} \tag{2}$$

where, $q(x)$: heat flux (W/cm^2)

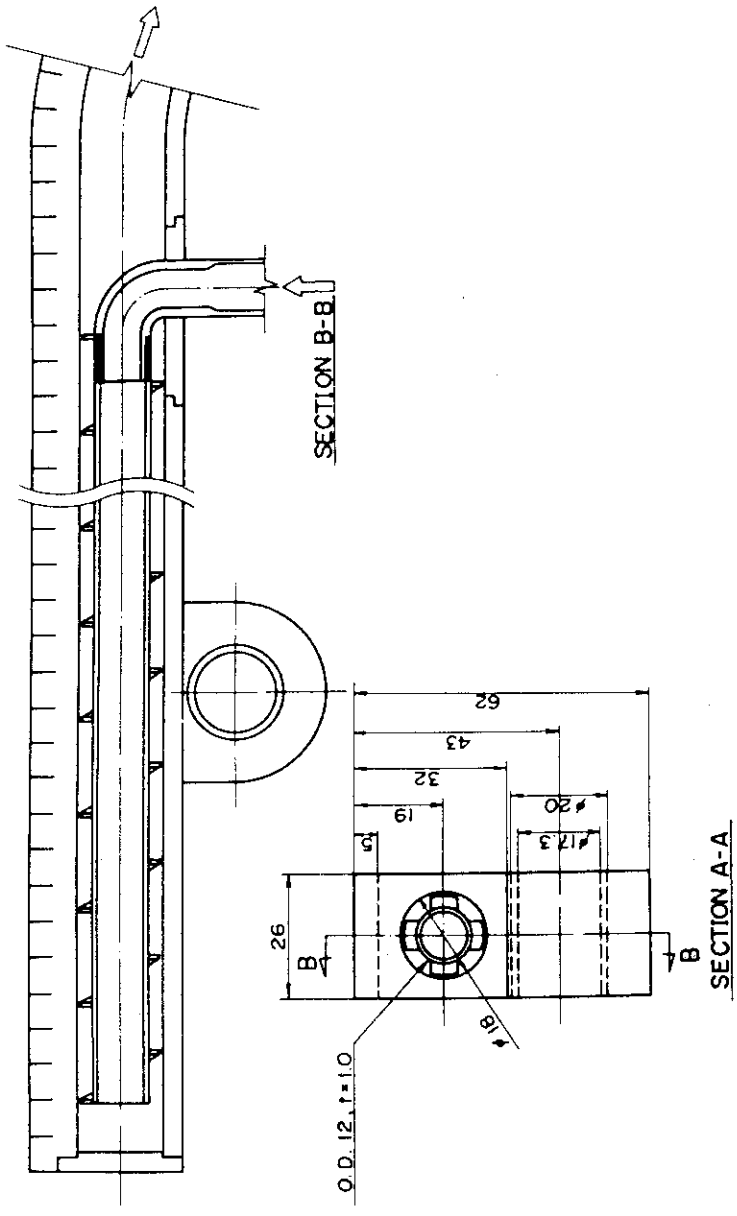

Fig.3 Detailed Cross Section View of Divertor Collector Plate

Table 1 Design Conditions and Design Parameters of Divertor Plates

Type	Co-axial tube assembly
Material	
cooling tube	Copper
armor	Tungsten
Heating	
total surface heat flux	40 MW
total deposition heat	10 MW
maximum heat flux	2.6 MW/cm^2 at outer plate
	1.6 MW/m^{22} at inner plate
beam angle to plate	40° at outer plate
	40° at inner plate
heat deposition rate	6 W/cc
Coolant	
temperature of coolant	60/70°C
pressure of coolant	1.5/1.2 MPa
inlet velocity	5 m/sec
pressure drop	0.3 MPa
Particle flux	
total particle flux	1×10^{23}/sec
maximum ion flux density	$5.9 \times 10^{21}/m^2 \cdot sec$ at outer plate
	$3.4 \times 10^{21}/m^2 \cdot sec$ at inner plate
beam width of half magnitude	10cm & 5cm at outer plate
	10cm at inner plate

q_{max} : maximum heat flux (W/cm^2)
$\varphi(x)$: particle flux density ($1/m^2 \cdot sec$)
φ_{max} : maximum ion flux density ($1/m^2 \cdot sec$)
Δ : beam width of a half magnitude (cm)
x : distance from the center line of ion beam (cm)

Total surface heat flux and total particle flux are respectively obtained by integrating equation (1) and (2) in the longitudinal and torus directions. They are estimated to be 40 MW and $1 \times 10^{23}/s$, respectively. A distribution between upper and lower divertor, and that between the inner and outer plates are assumed to be same values of INTOR[5], and to be 1 : 1 and 1 : 3, respectively. Assuming the beam widths of a half magnitudes are 10 cm and 5 cm for the outer plate and 10 cm for the inner plate, the maximum heat fluxes on the inner and outer plates are 240 W/cm^2 and 410 W/cm^2, respectively. To take into account the inclination of beam to the plate and major radius of the plates, these become 154 W/cm^2 and 260 W/cm^2. Similarly, the maximum ion flux densities on the inner and outer plates are $3.44 \times 10^{21}/m^2 \cdot sec$ and $5.9 \times 10^{21}/m^2 \cdot sec$, respectively.

The main design conditions and design parameters of the divertor plates are shown in Table 1.

3. Thermal analysis

Since the heat loads on the outer plate are larger than those on the inner plate, thermal and stress analyses are performed only for the outer plate. Thermal analysis is conducted under the conditions shown in Table 1.

3.1 Temperature distribution of the coolant

The coolant has its temperature distribution in a longitudinal direction because of its flow effect and the distribution of the heat flux in the longitudinal direction. The coolant temperatures in the inner and outer tubes are different even in the same position.
The relations of the heat transfer between the coolants in the inner and outer tubes are approximately given by the following equations.

$$h_2 k_2 (\varphi_2 - \varphi_1) - C_p G \frac{d\varphi_1}{dx} = 0 \tag{3}$$

$$h_q \cdot q + h_1 k_1 (\varphi_1 - \varphi_2) + C_p G \frac{d\varphi_2}{dx} = 0 \tag{4}$$

q_{max} : maximum heat flux (W/cm^2)
$\varphi(x)$: particle flux density ($1/m^2 \cdot sec$)
φ_{max} : maximum ion flux density ($1/m^2 \cdot sec$)
Δ : beam width of a half magnitude (cm)
x : distance from the center line of ion beam (cm)

Total surface heat flux and total particle flux are respectively obtained by integrating equation (1) and (2) in the longitudinal and torus directions. They are estimated to be 40 MW and 1×10^{23}/s, respectively. A distribution between upper and lower divertor, and that between the inner and outer plates are assumed to be same values of INTOR[5], and to be 1 : 1 and 1 : 3, respectively. Assuming the beam widths of a half magnitudes are 10 cm and 5 cm for the outer plate and 10 cm for the inner plate, the maximum heat fluxes on the inner and outer plates are 240 W/cm^2 and 410 W/cm^2, respectively. To take into account the inclination of beam to the plate and major radius of the plates, these become 154 W/cm^2 and 260 W/cm^2. Similarly, the maximum ion flux densities on the inner and outer plates are $3.44 \times 10^{21}/m^2 \cdot sec$ and $5.9 \times 10^{21}/m^2 \cdot sec$, respectively.

The main design conditions and design parameters of the divertor plates are shown in Table 1.

3. Thermal analysis

Since the heat loads on the outer plate are larger than those on the inner plate, thermal and stress analyses are performed only for the outer plate. Thermal analysis is conducted under the conditions shown in Table 1.

3.1 Temperature distribution of the coolant

The coolant has its temperature distribution in a longitudinal direction because of its flow effect and the distribution of the heat flux in the longitudinal direction. The coolant temperatures in the inner and outer tubes are different even in the same position. The relations of the heat transfer between the coolants in the inner and outer tubes are approximately given by the following equations.

$$h_2 k_2 (\varphi_2 - \varphi_1) - C_p G \frac{d\varphi_1}{dx} = 0 \tag{3}$$

$$h_q \cdot q + h_1 k_1 (\varphi_1 - \varphi_2) + C_p G \frac{d\varphi_2}{dx} = 0 \tag{4}$$

where, φ : bulk temperature of coolant (°C)

h : heated perimeter (m)

k : over-all coefficient of heat transmission (kcal/m^{2}h)

q : heat flux (kcal/m^{2}h)

G : mass flow rate of liquid (kg/h)

C_p : specific heat of liquid (kcal/kg·°C)

x : distance from the center line of ion beam (m)

Suffix "1" and "2" indicate the inner tube and outer tube, respectively.

The temperature distribution of the coolant obtained from these equations is shown in Fig.5. The bulk coolant temperatures at the

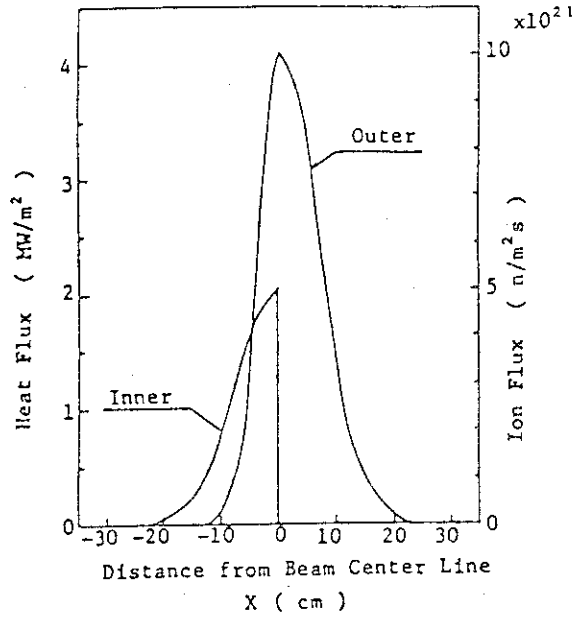

Fig.4 Heat Flux and Ion Flux Distribution (Normal to Separatrix)

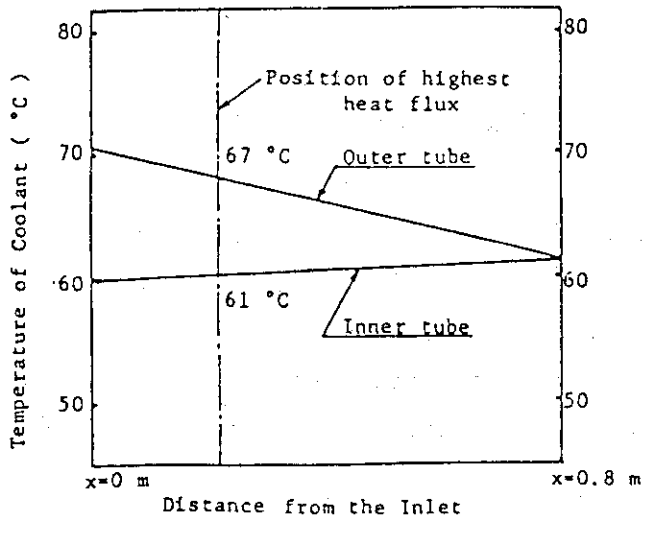

Fig.5 Temperature Distribution of Coolant in a Longitudinal Direction (Outer Plate)

position of the highest heat flux are estimated to be 61°C in the inner tube and 67°C in the outer tube, respectively. These temperatures are a little under-estimated since this simple calculation does not take into account the increase of the heat transfer coefficient by the boiling of the coolant.

The inlet pressure of the coolant is tentatively set to be 1.5 MPa to avoid the excessive boiling. Total pressure drop of the coolant in the divertor plate is sum of those in the inner straight tube, at the end of the co-axial tube where coolant changes its flow direction and in the outer straight tube. The coolant in the outer tube is predicted to be partially two phase flow with boiling while others are single phase flow. However, the detailed calculations of these pressure losses are very complicated except that in the inner straight tube so that total pressure drop of the coolant is conservatively assumed to be 0.3 MPa in this study. This value is largely over-estimated because total pressure loss in the inner and outer straight tubes without boiling becomes about 0.1 MPa. Then, the coolant pressures at the position of the highest heat flux are assumed to be 1.5 MPa in the inner tube and 1.2 MPa in the outer tube, respectively.

The detailed calculation of the pressure losses are required in the future.

3.2 Selection of boiling curve

Since the director plates receive very high heat flux from the plasma, the coolant in the tube is predicted to boil partially. If a cooling system without boiling of the coolant is employed by increasing the pressure and flow rate of the coolant, the cooling system of the divertor plates has a disadvantage from the stand point of economic design. Such cooling parameters increase pressure drop and hence its circulating power. Therefore, it is important for the thermal design of the divertor plates to predict a boiling curve of the coolant.

The commonly used design procedures for predicting a boiling curve from existing data are depicted in Fig.6[6], which were proposed by McAdams, et al.[7], Kutateladze[8], Rohsenow[9] and Engelberg-Forster and Grief[10]. These curves indicate the relation of the heat flux on the cooling surface, q and the difference of wall and saturation temperatures, $(T_w - T_s)$.

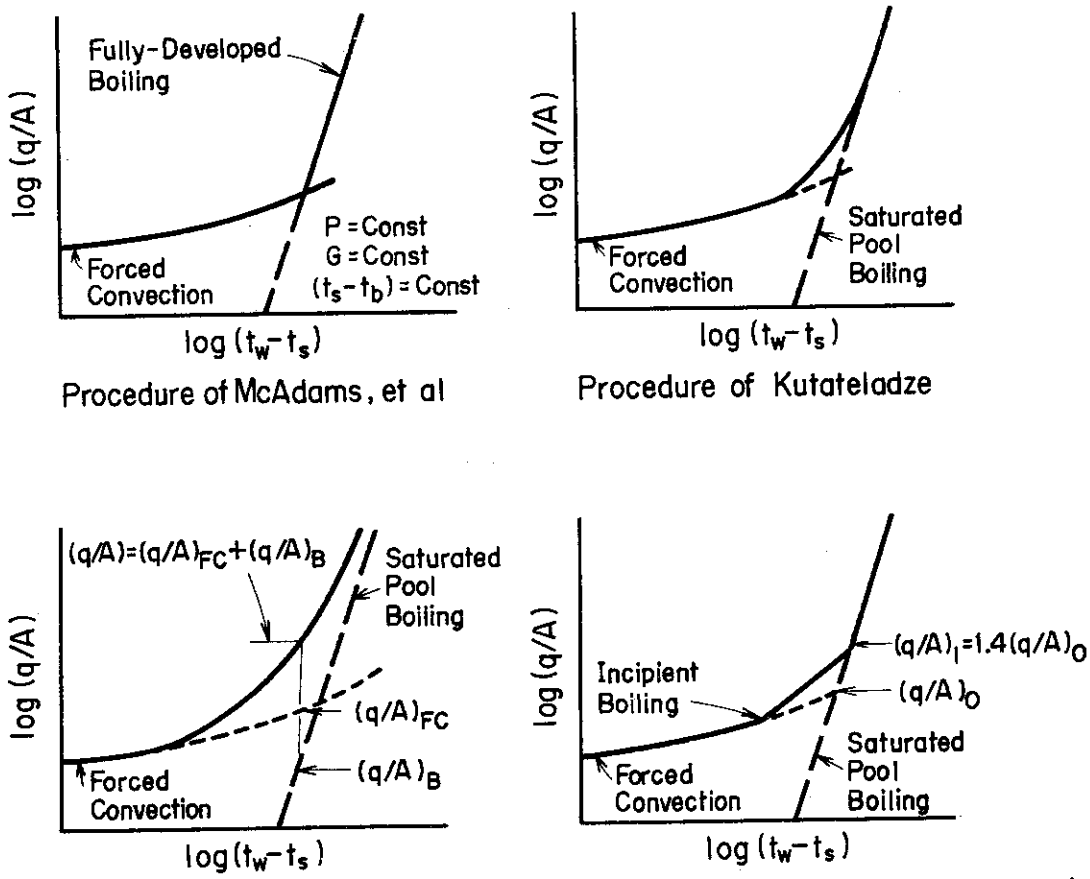

Fig.6 Procedures for estimation of heat transfer with forced-convection surface boiling

where, T_w : wall temperature (°C)

T_s : saturation temperature of coolant (°C)

Three distinct regions are found in forced-convection surface boiling. At low wall superheat, the heat transfer is governed by forced convection. At moderate wall superheat the heat transfer is determined by the combined effects of forced convection and surface boiling. At higher wall superheat the effect of forced convection disappears and fully developed boiling governs heat transfer.

The procedure of Mcadams, et al. seems to be considerable under-estimation and that of Rohsenow to be over-estimation for the thermal design of the divertor plates, since the coolant of the divertor plates is used at the moderate wall superheat. The concept of incipient boiling is not included in the procedure of Kutateladze. Then, the procedure of Engelberg-Forster and Grief is employed for the boiling curve in this analysis.

This boiling curve indicates that the correlation of nonboiling forced-convection and pool boiling for the coolant are required. The intersection of the two equations give a heat flux q_0. An empirical relation is used to locate the point where the boiling curve is essentially the same as for the pool boiling; $q_1 = 1.4\ q_0$.[10] The region between incipient boiling and q_1 is represented by a straight line.

It is not known, however, how the point of incipient boiling is determined. The formula of Rohsenow, employed for estimating the incipient boiling, is as follow[11]:

$$q_i = 911\ p^{1.156}\ \left[(T_w - T_s) \times \frac{9}{5}\right]^{\left(\frac{2.30}{p^{0.0234}}\right)} \qquad (5)$$

where, q_i : heat flux of incipient boiling (kcal/m^{2}h)

p : coolant pressure (ata)

The point of incipient boiling on the curve is obtained from the intersection between the forced convection equation and the above-mentioned equation of Rohsenow. The formulas of Jens and Lottes are used for fully developed boiling as follows[11];

$$T_w - T_s = 0.82\ q^{1/4}\ e^{-\frac{P}{63}} \qquad (6)$$

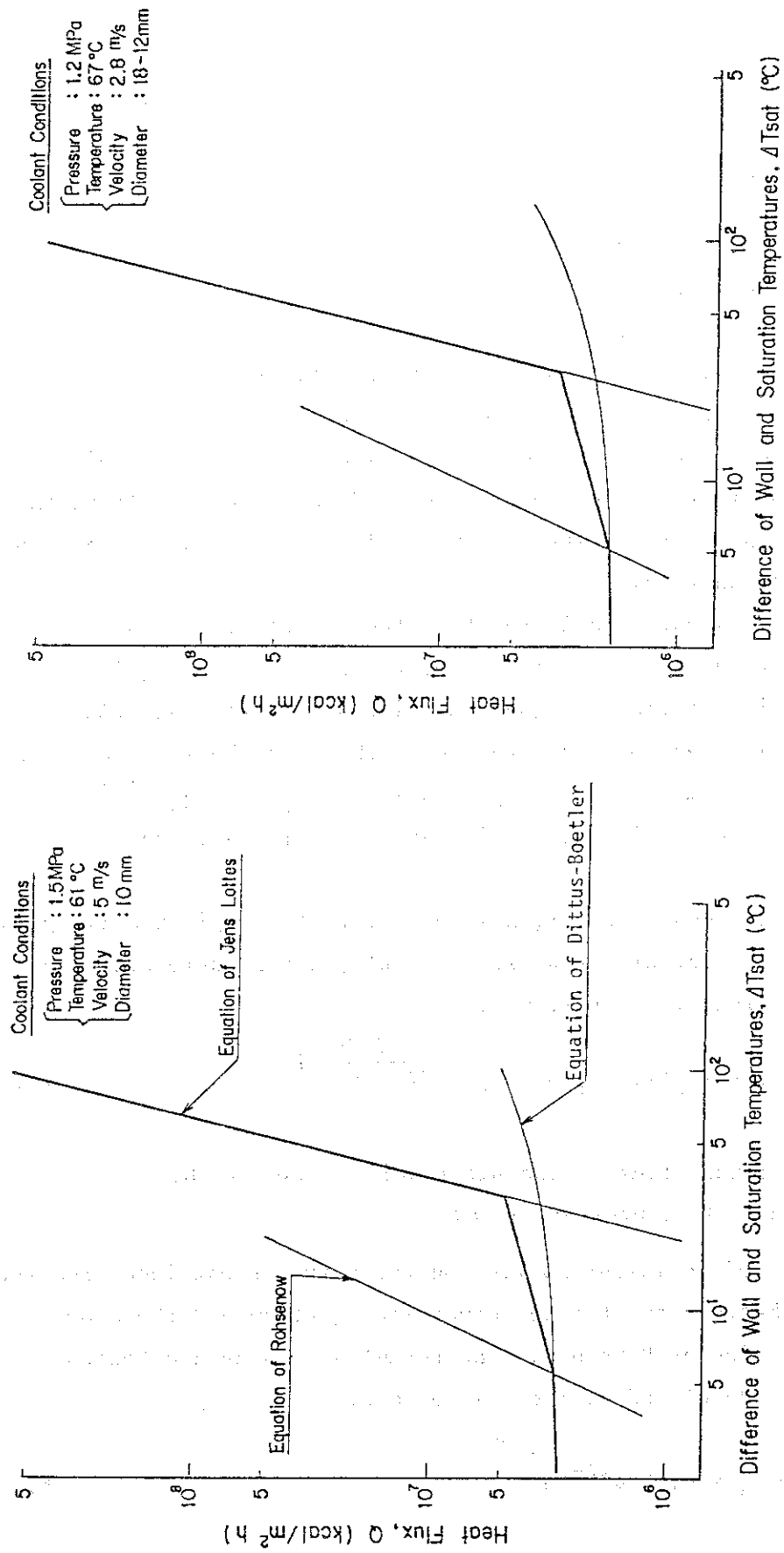

Fig. 7 Boiling Curve of Cooling Water in Inner Tube

Fig.8 Boiling Curve of Cooling Water in Outer Tube

The formula of Dittus-Boetler is employed to obtain a heat transfer of nonboiling forced-convection. As the result, the boiling curves used in this analysis for the inner and outer tube are depicted in Figs.7 and 8, respectively.

3.3 Two dimensional thermal analysis

A two dimensional transient thermal analysis in the cross section of the highest heat flux is carried out on the base of the obtained boiling curves using the finite element method. The heat transfer coefficients on the cooling surface vary along the boiling curves every time step, when the temperature on the cooling surface becomes more than saturation temperature of the coolant.

Figure 9 shows the thermal calculational model. The model includes only a half of the plate because of its symmetrical heat load. Figure 10 depicts the steady state temperature distributions of the divertor plate 20 seconds after the beginning of plasma burn. Time variations of the maximum temperatures of the armor, the copper tube and the cooling surface are illustrated in Fig.12. These steady state temperatures are reached about 15 seconds after the beginning of plasma burn. They are estimated to be 292°C on the plasma-side surface of the armor, 208°C on the brazing region of the copper tube and 202°C on the plasma-side surface in the outer cooling tube, respectively.

Since the saturation temperature of the cooling water at the pressure of 1.2 MPa is 187°C, the coolant partially boils on the cooling surface. Maximum heat flux on the cooling surface becomes 0.275 kW/cm^2, which is a little larger than the heat flux on the armor's surface from plasma, 0.26 kW/cm^2. This difference is due to boiling effect of the coolant and shaping effect of the coolant path with a circular cross section. Figure 11 shows the temperature distribution of the divertor plate when the boiling of the coolant is not taken into account. From comparison of Fig.10 and 11, the maximum temperature on the cooling surface in the case of nonboiling is about 10°C higher than that in the case of boiling. The maximum temperature of the armor in the case of nonboiling is also higher about same magnitude than that of boiling.

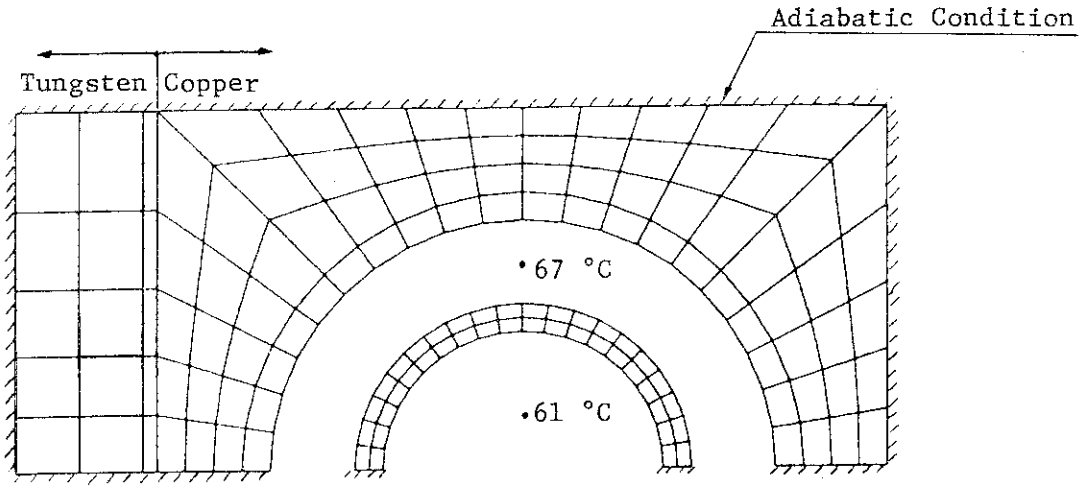

Fig.9 Thermal Calculational Model of Divertor Plate

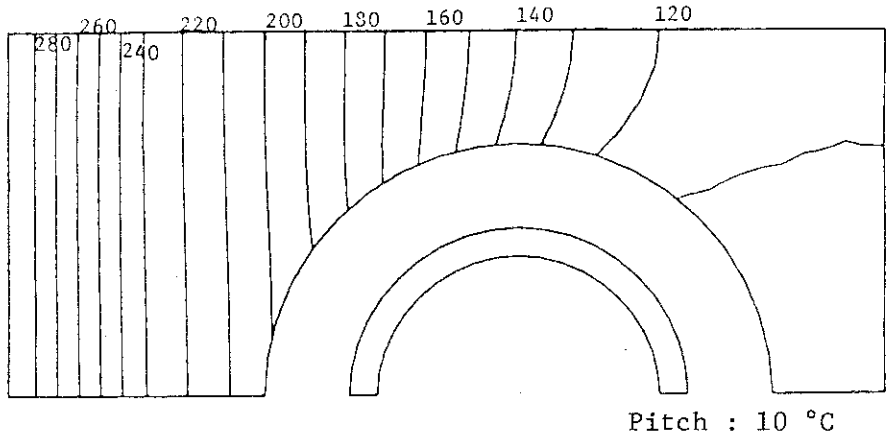

Fig.10 Temperature Distribution of Divertor Plate
(In the case of Boiling, Time= 20 sec)

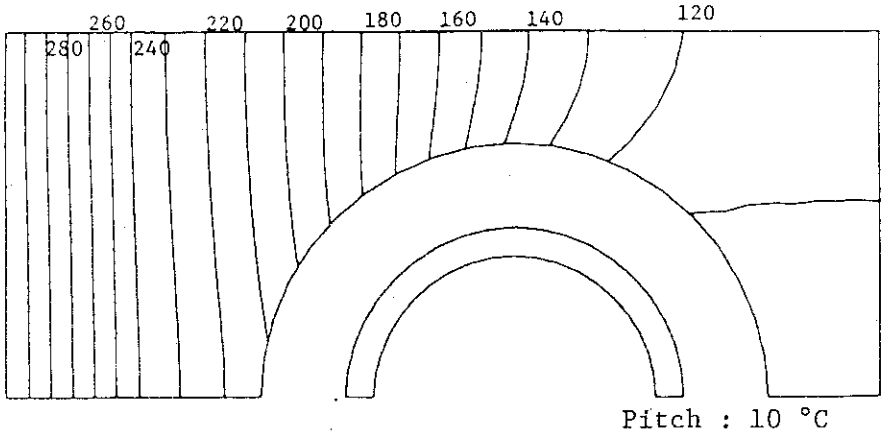

Fig.11 Temperature Distribution of Divertor Plate
(In the case of Non-boiling, Time= 20 sec)

3.4 Burn-out heat flux

A cooling system in which the coolant is boiled is reasonable for the effective removal of the high heat flux. The heat flux on the cooling surface, however, must be sufficiently lower than the burn-out heat flux. The burn-out heat flux can be obtained from the formulas proposed by several authors, Jens & Lottes, Zenkevich, Griffith and Rohsenow etc.

In this report, the burn-out heat flux is calculated using the formulas of P. Griffith which can be applied under the condition with the relatively wide pressure range. These formulas are given as follows[12],

$$q_{BO} = \frac{f_1(P/P_c)}{41.5} (i_{vs} - i_\ell)\gamma_v (g\nu_\ell)^{1/3} P_{r\ell}^{-2/3} \left(\frac{\gamma_\ell - \gamma_v}{\gamma_\ell}\right)^{1/3} f_2^* \quad (7)$$

$$f_2^* = 1 + 10^{-6} R_{e\ell} + 0.0144 S + 0.5 \times 10^{-3} [R_{e\ell} \cdot S]^{1/2}$$

$$R_{e\ell} = \frac{u \cdot D}{\nu_\ell} \quad , \qquad S = \frac{C_\ell \Delta T_{sub}}{L} \left(\frac{\rho_\ell}{\rho_v}\right)$$

where,
- q_{BO} : burn-out heat flux (kcal/m^{2}h)
- f_1 : pressure function (see Fig.13)
- P : coolant pressure (ata)
- P_c : critical pressure of coolant (ata)
- i_{vs} : enthalpy of saturated vapor (kcal/kg)
- i_ℓ : enthalpy of liquid (kcal/kg)
- L : latent heat of vaporization (kcal/kg)
- γ_v : specific weight of saturated vapor (kg/m^3)
- γ_ℓ : specific weight of saturated liquid (kg/m^3)
- g : acceleration of gravity (m/sec^2)
- ν_ℓ : kinematic viscosity of liquid (m^2/sec)
- $R_{e\ell}$: Reynolds number of liquid
- $P_{r\ell}$: Prandtl number of liquid
- u : coolant velocity (m/sec)
- D : hydraulic diameter (m)
- C_ℓ : specific heat of liquid (kcal/kg·°C)
- ΔT_{sub} : subcooling (= $T_s - T_\ell$) (°C)
- ρ_v : mass density of saturated vapor (kg·sec^2/m^4)
- ρ_ℓ : mass density of saturated liquid (kg·sec^2/m^4)

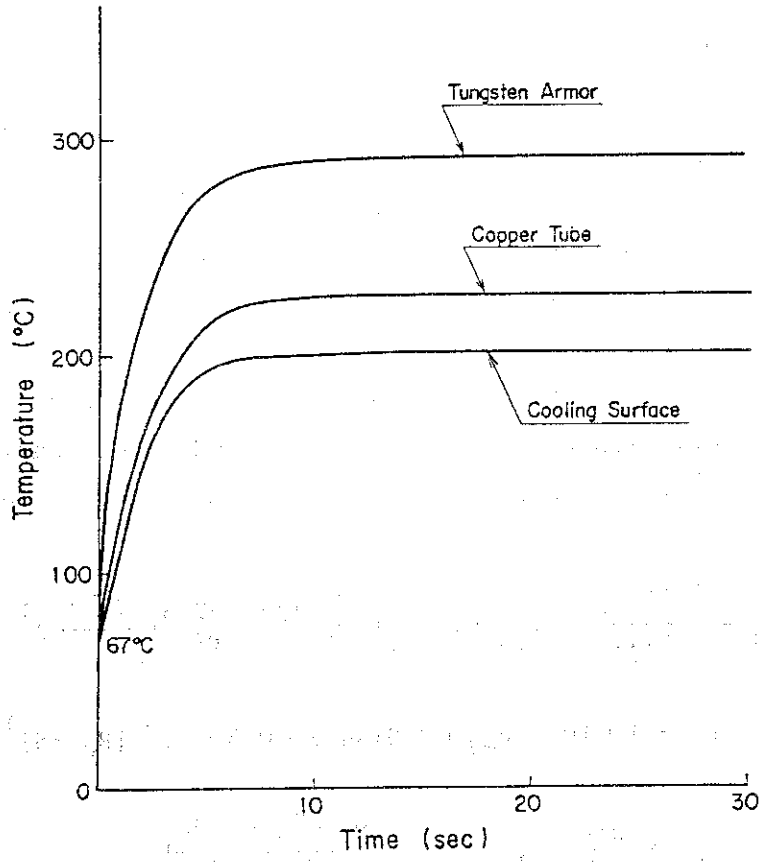

Fig.12 Time Variations of Maximum Temperatures of Armor, Copper Tube and Cooling Surface

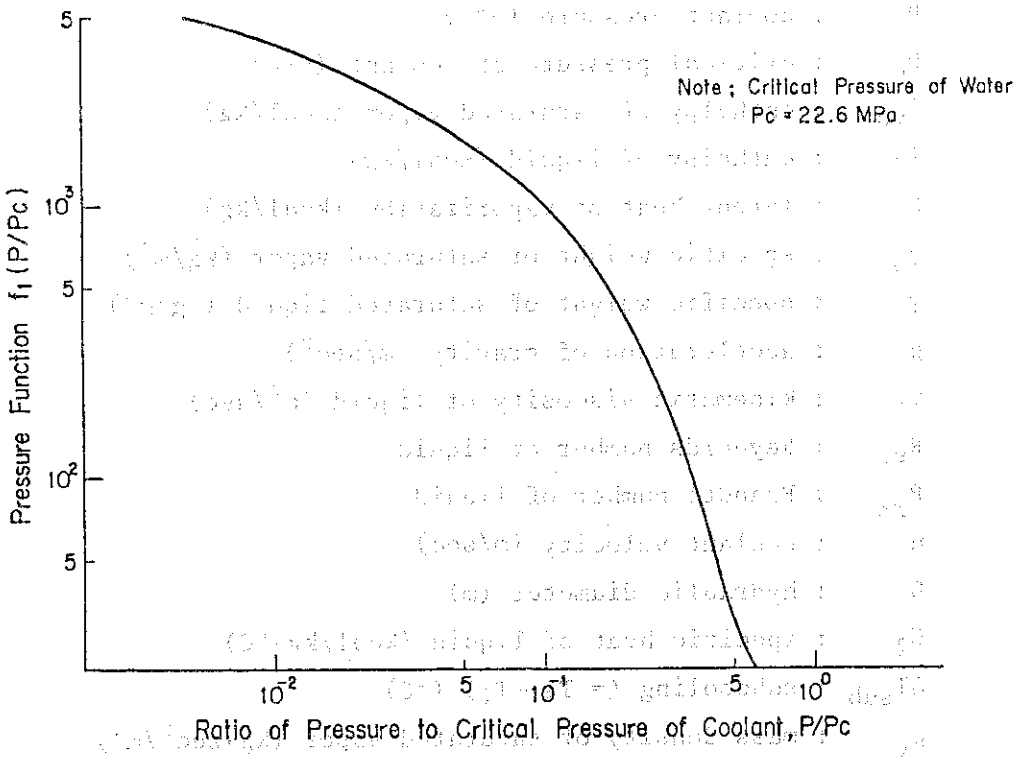

Fig.13 Value of Pressure Function, f1 (P/Pc)

T_s : saturation temperature of coolant (°C)

T_ℓ : coolant temperature (°C)

According to the formulas of P. Griffith, the burn-out heat flux is estimated to be 1.08 ± 0.36 kW/cm^2. Since these formulas include the error of about ±33%, upper and lower limits of the burn-out heat flux are estimated to be 1.44 kW/cm^2 and 0.72 kW/cm^2, respectively. The maximum heat flux on the cooling surface of 0.275 kW/cm^2 is sufficiently below the lower limit of the burn-out heat flux.

4. Stress analysis

The forces acting on the divertor plate during the operation are considered to be thermal stresses caused by the heat load from plasma and the electromagnetic force in the case of the plasma disruption. Internal hydraulic pressure acts on the cooling tube but the stress caused by the pressure is small enough in comparison with above forces. Since magnetic flux on each area encircled by the electrical loop on the plate is very small compared to the convensional type divertor plate, the electromagnetic force in the case of plasma disruption is also negligibly small. The thermal stresses are caused by the temperature distribution in the cross section of the plate and the temperature distribution in the longitudinal direction.

In this report, the thermal stress caused by the temperature distribution in the cross section of the plate is analyzed without taking into account that in the longitudinal direction in order to approximately evaluate the strength of the plate. The detailed three dimensional stress analysis, however, should be studied in the future taking into account both the temperature distributions in the cross section and in the longitudinal direction.

4.1 Two dimensional stress analysis

Two dimensional thermal stress analysis (plane stress analysis) with the temperature distribution shown in Fig.10 is carried out by means of the finite element code, SAP-V.

Figure 14 illustrates the calculational model of the stress analysis. All the nodal points on the center line are fixed in Z direction as shown in Fig.14 because of the symmetrical temperature distribution. Figure 15 shows the pre- and post-deformation shapes

T_s : saturation temperature of coolant (°C)

T_ℓ : coolant temperature (°C)

According to the formulas of P. Griffith, the burn-out heat flux is estimated to be 1.08 ± 0.36 kW/cm^2. Since these formulas include the error of about ±33%, upper and lower limits of the burn-out heat flux are estimated to be 1.44 kW/cm^2 and 0.72 kW/cm^2, respectively. The maximum heat flux on the cooling surface of 0.275 kW/cm^2 is sufficiently below the lower limit of the burn-out heat flux.

4. Stress analysis

The forces acting on the divertor plate during the operation are considered to be thermal stresses caused by the heat load from plasma and the electromagnetic force in the case of the plasma disruption. Internal hydraulic pressure acts on the cooling tube but the stress caused by the pressure is small enough in comparison with above forces. Since magnetic flux on each area encircled by the electrical loop on the plate is very small compared to the convensional type divertor plate, the electromagnetic force in the case of plasma disruption is also negligibly small. The thermal stresses are caused by the temperature distribution in the cross section of the plate and the temperature distribution in the longitudinal direction.

In this report, the thermal stress caused by the temperature distribution in the cross section of the plate is analyzed without taking into account that in the longitudinal direction in order to approximately evaluate the strength of the plate. The detailed three dimensional stress analysis, however, should be studied in the future taking into account both the temperature distributions in the cross section and in the longitudinal direction.

4.1 Two dimensional stress analysis

Two dimensional thermal stress analysis (plane stress analysis) with the temperature distribution shown in Fig.10 is carried out by means of the finite element code, SAP-V.

Figure 14 illustrates the calculational model of the stress analysis. All the nodal points on the center line are fixed in Z direction as shown in Fig.14 because of the symmetrical temperature distribution. Figure 15 shows the pre- and post-deformation shapes

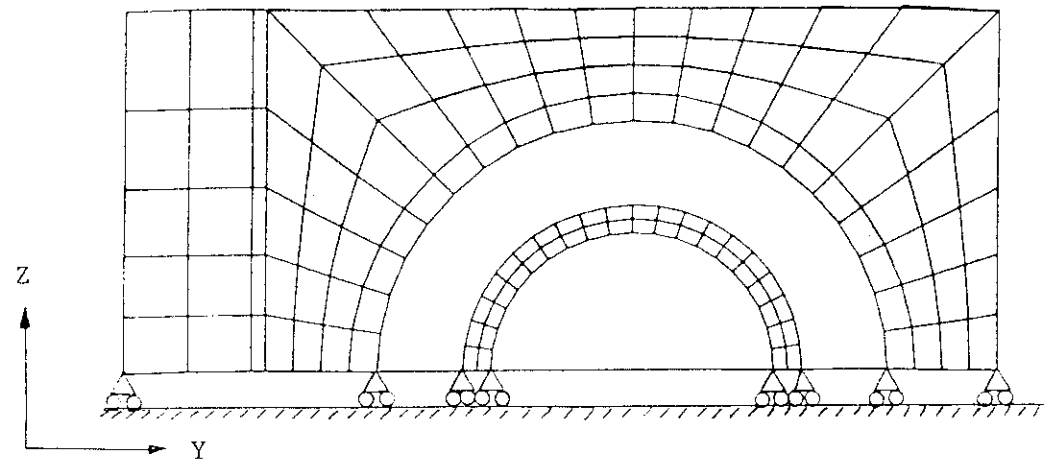

Fig.14 Stress Calculational Model of Divertor Plate

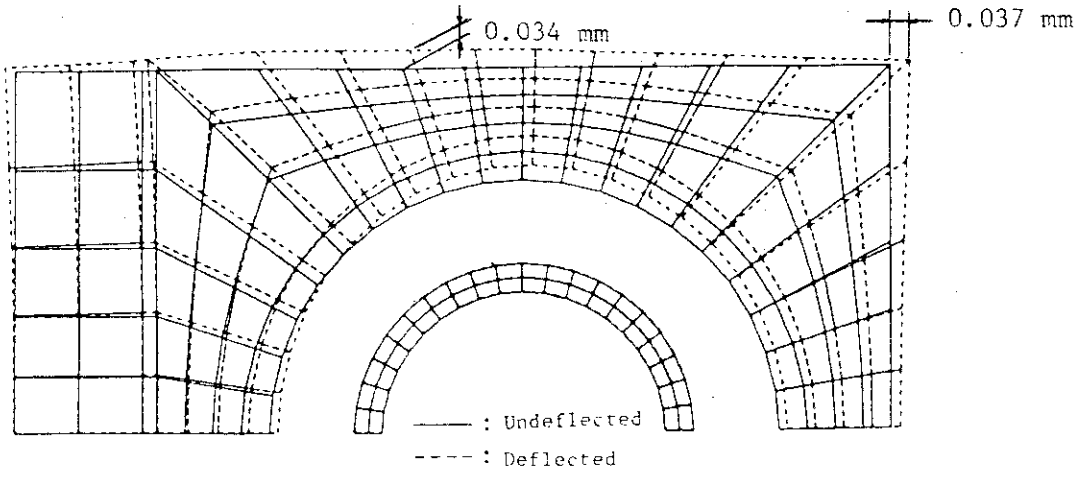

Fig.15 Pre- and Post-Deformation Shapes of Divertoe Plate
(Time = 20 sec)

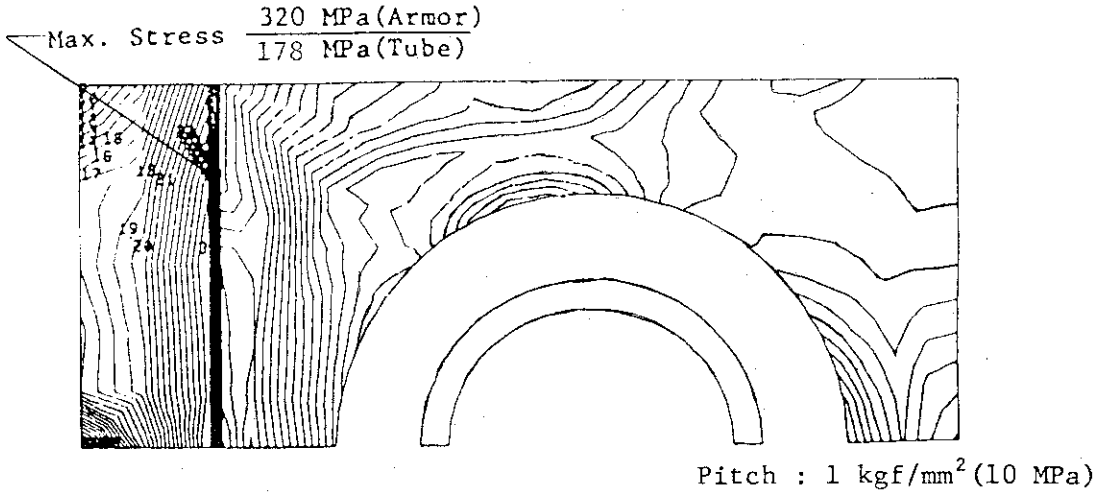

Fig.16 Stress Intensity Distribution of Divertor Plate
(Time = 20 sec)

under the temperature distribution shown in Fig.10. Maximum displacements of the plate are estimated to be 0.037 mm in Y direction and 0.034 mm in Z direction, respectively. The displacements of the plate due to the temperature distribution in the cross section are so small that the increase of the heat flux to the plate due to the deformation of the plate is negligible. Figure 16 depicts the stress intensity distribution of the divertor plate 20 seconds after the beginning of plasma burn. The maximum stress intensities of the armor and copper tube appear at the brazed point due to the difference of thermal expansion between tungsten and copper. They are estimated to be 320 MPa and 178 MPa, respectively.

4.2 Stress evaluation

The stresses in the copper tube and tungsten armor are evaluated by employing ASME Code Sec.Ⅲ[12].

The yield strength of tungsten at the temperature of 300°C is 490 MPa and that of copper (OFHC-0.2% Ag) at 200°C is 69 MPa. Allowable stresses of both materials against the thermal stress, which corresponds to $(P_L + P_b + Q)$ in ASME Code Sec.Ⅲ, become 980 MPa and 137 MPa, respectively.

Maximum stress intensity of the tungsten armor (320 MPa) is sufficiently below the allowable limit (980 MPa) and it can be said that the armor has enough margin of strength against failure. Maximum stress intensity of the copper tube (178 MPa), however, exceeds the allowable limit (137 MPa) so that fatigue analysis must be carried out for the copper stress. Figure 17 illustrates the fatigue curves of copper (OFHC-0.2% Ag) at the temperature of 200°C[13]. Since there are not fatigue data of annealed copper, data of copper with 20% cold reduction is tentatively used. Dotted line shows experimental fatigue data and solid line shows design fatigue curve which is derived conservatively from the experimental data. In fatigue analysis, solid line should be employed. Stress range shown in Fig.17 corresponds to a half magnitude of cyclic stress intensity.

From Fig.17, allowable cycles for the maximum stress intensity of the copper tube are estimated to be about 10^4 cycles. These cycles correspond to the life time of about 4 months. Therefore, some measures are required to decrease the thermal stress for extending the life time

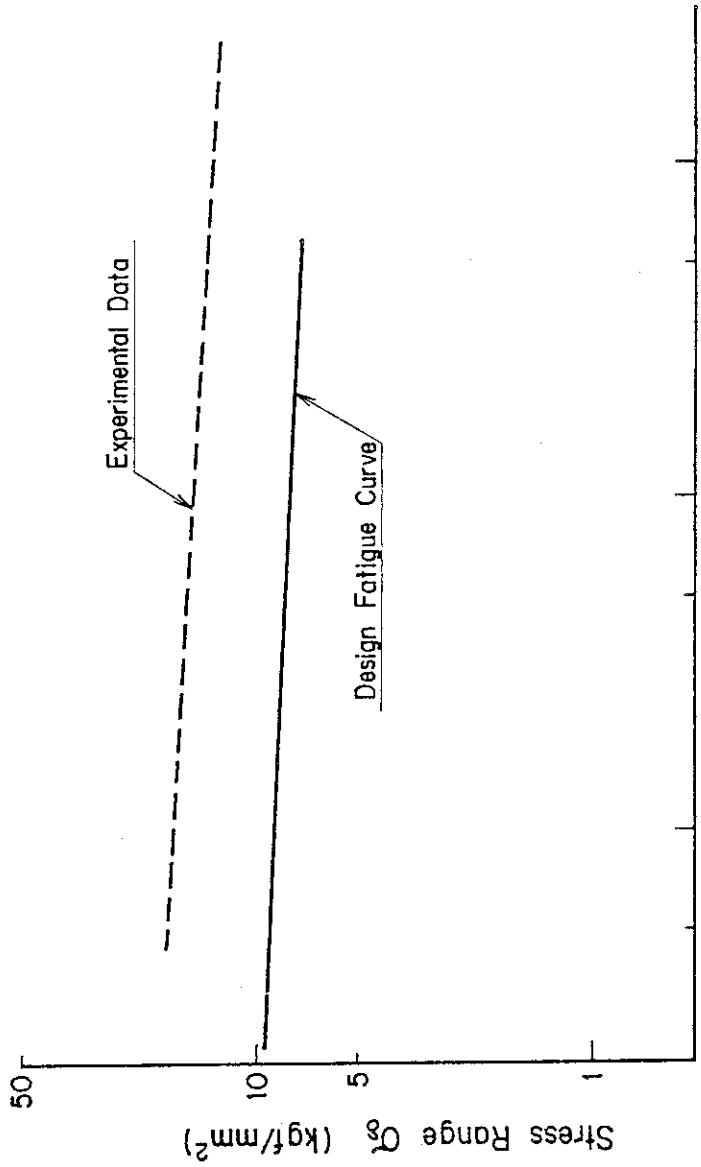

Fig. 17 Fatigue Curve of Copper (0.2% Ag. Cu) at 200°C.

of the plate. These will be, for example, decreasing the heat flux on the plate by the reduction of the beam angle to the plate, reducing the coolant pressure, or developing the new material which has high thermal conductivity and mechanical strength in place of copper.

5. Estimation of life time by ion sputtering

The divertor plate surface is eroded by the charged particles. Armor made of tungsten is employed here because of its small erosion rate by the ion sputtering, the high heat conductivity and the large mechanical strength in the high temperature region. The life time of the divertor plates by the erosion due to ion sputtering is estimated approximately.

The erosion rate of tungsten is given by followings[14],

$$\dot{x} = \frac{A_V M}{N_0 \rho} \varphi_{max} \eta \qquad (8)$$

where, $\dot{x}$: erosion rate (cm/sec)
A_V : availability (= 0.25)
M : atomic weight of tungsten (= 184)
N_0 : Avogadro's number (= 6.02×10^{23})
ρ : mass density of tungsten (= 19.3 g/cm^3)
φ_{max} : maximum ion flux density (n/cm^2·sec)
η : sputtering yield of tungsten

The maximum ion flux densities are previously obtained to be 5.9×10^{21}/m^2·sec on the outer plate and 3.44×10^{21}/m^2·sec on the inner plate, respectively. The sputtering yield of 2.24×10^{-3} atom/ion for tungsten is employed here[5]. Assuming 0.25 of the reactor availability and 0.7 of the duty factor, the maximum erosion rates due to ion sputtering are estimated to be 3.66×10^{-8} mm/sec for the outer plate and 2.13×10^{-8} mm/sec for the inner plate, respectively. Taking into account the armor thickness of 5 mm, the life time of the divertor plates are estimated to be 4.33 years for the outer plate and 7.44 years for the inner plate, respectively.

These values seem to be reasonable for the life time of the divertor plates even considering the complexity of repair and maintenance of the plates.

of the plate. These will be, for example, decreasing the heat flux on the plate by the reduction of the beam angle to the plate, reducing the coolant pressure, or developing the new material which has high thermal conductivity and mechanical strength in place of copper.

5. Estimation of life time by ion sputtering

The divertor plate surface is eroded by the charged particles. Armor made of tungsten is employed here because of its small erosion rate by the ion sputtering, the high heat conductivity and the large mechanical strength in the high temperature region. The life time of the divertor plates by the erosion due to ion sputtering is estimated approximately.

The erosion rate of tungsten is given by followings[14],

$$\dot{x} = \frac{A_V M}{N_0 \rho} \varphi_{max} \eta \qquad (8)$$

where, $\dot{x}$: erosion rate (cm/sec)
A_V : availability (= 0.25)
M : atomic weight of tungsten (= 184)
N_0 : Avogadro's number (= 6.02×10^{23})
ρ : mass density of tungsten (= 19.3 g/cm^3)
φ_{max} : maximum ion flux density (n/cm^2·sec)
η : sputtering yield of tungsten

The maximum ion flux densities are previously obtained to be 5.9×10^{21}/m^2·sec on the outer plate and 3.44×10^{21}/m^2·sec on the inner plate, respectively. The sputtering yield of 2.24×10^{-3} atom/ion for tungsten is employed here[5]. Assuming 0.25 of the reactor availability and 0.7 of the duty factor, the maximum erosion rates due to ion sputtering are estimated to be 3.66×10^{-8} mm/sec for the outer plate and 2.13×10^{-8} mm/sec for the inner plate, respectively. Taking into account the armor thickness of 5 mm, the life time of the divertor plates are estimated to be 4.33 years for the outer plate and 7.44 years for the inner plate, respectively.

These values seem to be reasonable for the life time of the divertor plates even considering the complexity of repair and maintenance of the plates.

6. Concluding remarks

The thermal and structural design of the divertor collector plates with the co-axial tubes assembly is conducted. The electromagnetic force on the divertor plates due to plasma disruption is negligible, since magnetic flux change on each area encircled by the electrical loop is very small in the co-axial tube type divertor plate.

Thermal analysis of the plates is performed taking into account the boiling of the coolant. The procedure proposed by Engelberg-Forster and Grief is employed as the boiling curve of the coolant. The maximum heat flux on the cooling surface is sufficiently below the burn-out heat flux obtained from the formulas of P. Griffith.

Thermal stress analysis of the plate with the temperature distribution obtained by the thermal analysis is also conducted. The displacements of the plate due to the thermal load is very small so that the increase of the heat flux caused by the deformation of the plate is found to be negligible.

The maximum thermal stresses of the tungsten armor and the copper tube appear at the brazing region between both materials. The stress of the tungsten armor is estimated to be sufficiently below the allowable limit and that of the copper tube, however, a little exceeds the allowable limit against $(P_L + P_b + Q)$ in ASME code. Then, the fatigue analysis for the copper tube is performed. The life time of the divertor plate considering the cyclic thermal stress is estimated to be about 4 months. The life time of the plate due to ion sputtering is estimated to be 4.3 years, which is sufficiently longer in comparison with the life time due to thermal stress.

Therefore, some measures are required to decrease the thermal stress for extending the life time of the plate. These will be, for example, decreasing the heat flux on the plate by the reduction of the beam angle to the plate, reducing the coolant pressure, or developing the new material which has high thermal conductivity and mechanical strength in place of copper.

Figure 18 shows the maximum temperatures of the armor, copper tube and cooling surface, the burn-out heat flux and maximum heat flux on the cooling surface, as a function of the coolant pressure. Maximum stress intensities of the armor and copper tube as a function of the coolant pressure is shown in Fig.19. From Fig.19, the maximum stress

intensity of the copper tube would be below the allowable limit when the coolant pressure is 0.3 MPa.

As the design study presented here is in a preliminary stage, a more detailed design study about reducing method of the thermal stress should be carried out in the future. Furthermore, the following general features are also necessary to study in the future.

(i) Thermal and mechanical problems caused by the effect of the temperature difference in a longitudinal direction.

(ii) Propagation of the boiling region due to any disturbances during the operation.

(iii) Effects of material damage by neutron irradiation.

(iv) Selection of optimum coolant pressure.

(v) Thermohydraulic analysis of non-uniform coolant flow accompanied with partial boiling due to heat flux from one side and narrow coolant path.

Acknowledgement

Authors would like to thank Dr. M. Seki for his useful advice.

intensity of the copper tube would be below the allowable limit when the coolant pressure is 0.3 MPa.

As the design study presented here is in a preliminary stage, a more detailed design study about reducing method of the thermal stress should be carried out in the future. Furthermore, the following general features are also necessary to study in the future.

(i) Thermal and mechanical problems caused by the effect of the temperature difference in a longitudinal direction.

(ii) Propagation of the boiling region due to any disturbances during the operation.

(iii) Effects of material damage by neutron irradiation.

(iv) Selection of optimum coolant pressure.

(v) Thermohydraulic analysis of non-uniform coolant flow accompanied with partial boiling due to heat flux from one side and narrow coolant path.

Acknowledgement

Authors would like to thank Dr. M. Seki for his useful advice.

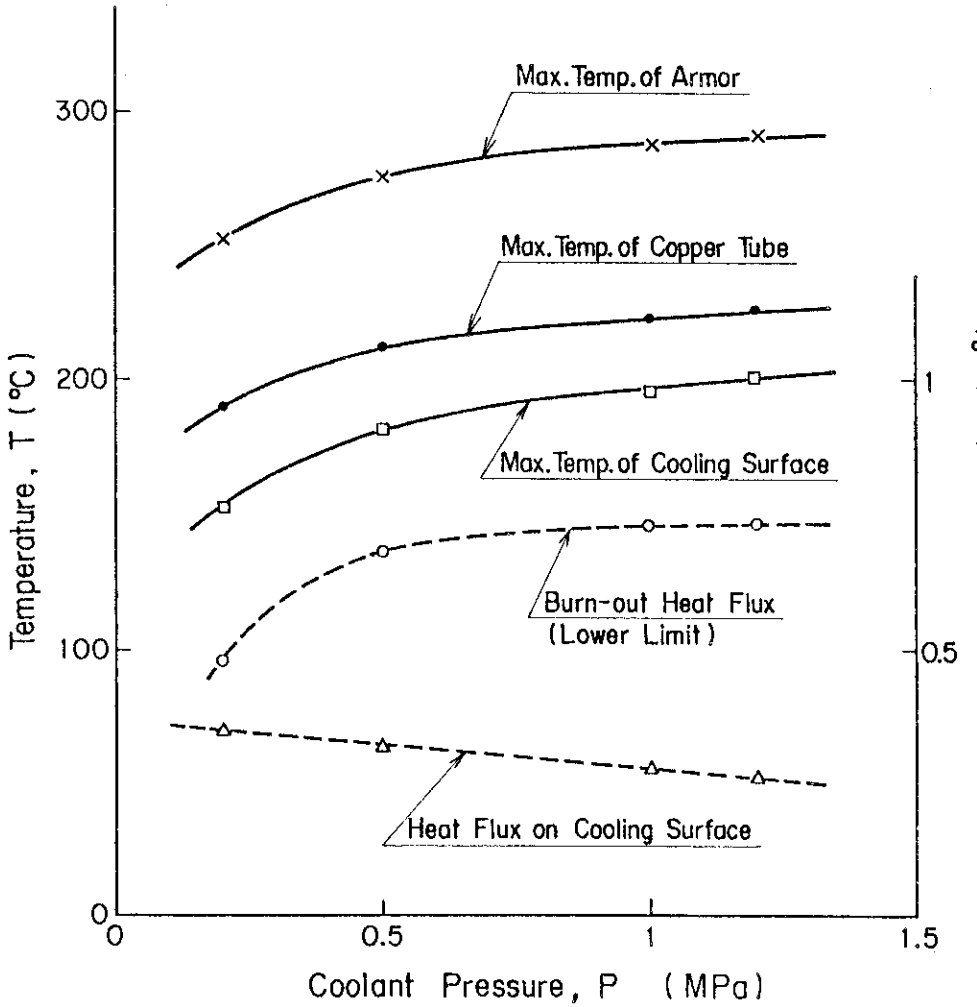

Fig. 18 Maximum Temperatures of Armor, Copper Tube and Cooling Surface and Burn-out Heat Flux and Max. Heat Flux on Cooling Surface as a function of coolant Pressure.

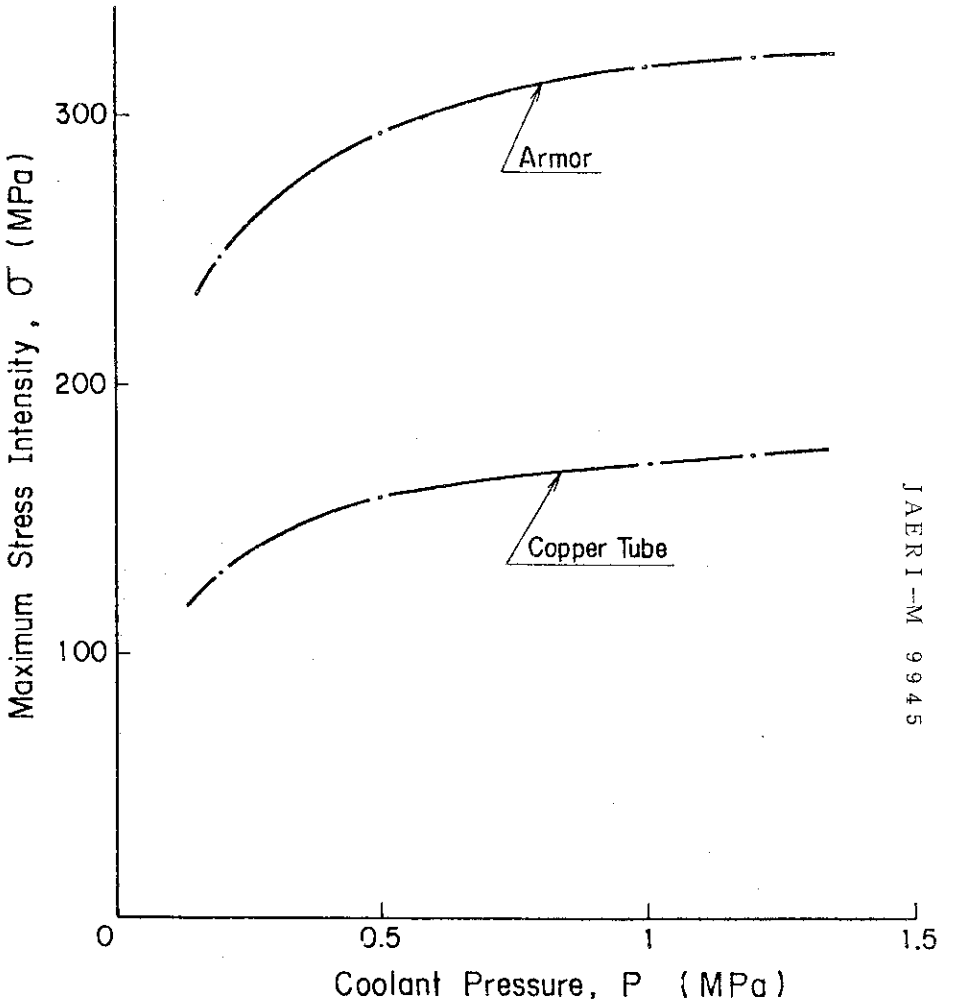

Fig. 19 Maximum Stress Intensities of Armor and Copper Tube as a function of Coolant Pressure.

References

[1] H. Iida et al., "Design Problem of High Heat Flux Divertor Structure", JAERI-M 8944 (1980)

[2] H. Iida et al., "Blanket and Vacuum Vessel Design of the Next Tokamak (Swimming Pool Type)", 3rd Technical Committe Meeting and Workshop on Fusion Reactor Design and Technology, Tokyo, 5-16 October, 1981

[3] K. Sako et al., "Next Tokamak Design (Swimming Pool Type)", 3rd Technical Committe Meeting and Workshop on Fusion Reactor Design and Technology, Tokyo, 5-16 October, 1981

[4] K. Sako et al., "A proposal of Swimming Pool Type Tokamak Reactor", JAERI-M 9025 (1980) in Japanese

[5] INTOR Phase I Final Report, Sec. IIV, June, 1981

[6] A.E. Bergles, W.M. Rohsenow, "The Determination of Forced-Convection Surface-Boiling Heat Transfer", Journal of Heat Transfer, Trans. ASME, Series C, Vol.86, 1964, PP.365-372

[7] W.H. McAdams, et al., "Heat Transfer at High Rates to Water with Surface Boiling", Industrial and Engineering Chemistry, Vol.41, 1949, PP.1945-1953

[8] S.S. Kutateladze, "Boiling Heat Transfer", International Journal of Heat Mass Transfer, Vol.4, 1961, PP.31-45

[9] W.M. Rohsenow, "Heat Transfer with Evaporation", Chapter in Heat Transfer, University of Michigan Press., 1953

[10] K. Engelberg-Forster and R. Greif, "Heat Transfer to a Boiling Liquid-Mechanism and Correlations", Journal of Heat Transfer, Trans. ASME, Series C, Vol.81, 1959, PP.43-53

[11] "Databook on Heat Transfer", JSME, 1975, in Japanese

[12] ASME Boiler and Pressure Vessel Code, Section III

[13] "Reliability of Main Components on JT-60", ISES-7904, Technical Research Association for INTEGRITY OF STRUCTURES AT ELEVATED SERVICE TEMPERATURES, March, 1979, in Japanese

[14] JAERI, "Conceptual Design Study Report of Next Tokamak Reactor (INTOR REFERENCE)", March, 1981, in Japanese